Earth-Atmosphere Angular Momentum Exchange and ENSO: The Rotational Signature of the 1997-98 Event

Jean O. Dickey[1], Pascal Gegout[1,2] and Steven L. Marcus[1]

1 Space Geodetic Science and Application Group
Jet Propulsion Laboratory
California Institute of Technology
Pasadena, CA 91109

2 Ecole et Observatoire des Sciences
de la Terre
Laboratoire de Dynamique Globale
67084 Strasbourg Cedex
France

Abstract

The impact of the 1997-1998 **ENSO event** is presented in context of Earth-atmosphere **angular momentum exchange** utilizing length of day (LOD), Southern Oscillation Index (SOI) and atmospheric angular momentum (AAM) data from 1970 to 1998; comparisons are made with previous events. The analysis of equal-area latitudinally belted AAM from the NCEP reanalysis (1958-98) reveals slow global coherent poleward propagation of angular momentum. These structures originate in the equatorial regions, penetrate into high latitudes and are bimodal in nature with variations centered at low-frequency (LF ~ 4.7 yr) and quasi-biennial (QB ~ 2.4 yr) periods. Analyses utilize both a recursive filter and multichannel singular spectrum analysis (M-SSA).

Introduction

The **El Niño Southern Oscillation** (ENSO), a climate fluctuation that recurs on a 2-7 yr. time scale, is associated with persistent large-scale variations in the dynamical behavior of the global **atmosphere-ocean system.** Comparisons between length of day (LOD, a measure of the Earth's axial rotation rate) and the strength of the ENSO cycle represented by the Southern Oscillation Index (SOI, the difference in sea level pressure between Darwin and Tahiti) have indicated striking agreement, with high interannual values of LOD generally coinciding with ENSO events (see *Chao*, 1984, 1988, 1989, *Eubanks et al.*, 1986; *Salstein and Rosen*, 1986; *Gambis*, 1992 and *Dickey et al.*, 1993 and 1994). During

an ENSO event, the SOI reaches a minimum, leading to an increase in atmospheric angular momentum (AAM) associated with the collapse of the tropical easterlies. Further increases in AAM may result from a strengthening of westerly flow in the subtropical jet streams. Conservation of total angular momentum then requires the Earth's rate of rotation to slow down, thus increasing LOD.

The ENSO event which began in early 1997 and persisted for approximately one year was one of the strongest ever recorded, both in terms of sea surface temperature (SST) anomalies in the eastern tropical Pacific and atmospheric circulation anomalies reflected in the SOI. The classical pattern of a deeper- and flatter-than-normal thermocline and low-level westerly winds in the tropical Pacific was accompanied by enhanced convection over the central and eastern tropical Pacific, with suppressed convection in the eastern Indian ocean and western Pacific modulated by strong activity of the Madden-Julian oscillation during the first half of 1997. The height of this episode was characterized by a complete collapse of the normal tropical low-level easterlies across the central and east-central equatorial Pacific, reflecting a persistent reversal of the equatorial Walker circulation. In this study, we examine the impact of this event on the global distribution of atmospheric angular momentum and the length-of-day, in the context of the atmosphere/solid Earth/ENSO connection over the last four decades.

Data and Techniques

The LOD series analyzed is the Jet Propulsion Laboratory (JPL) Kalman filtered series (sampled every 5 days) from 1970 to the end of 1997 (designated as COMB97; *R.S. Gross* [1998]) and LOD determined from JPL's operational Kalman filtered series for the year 1998. JPL's LOD series is derived from a Kalman filter-based combination of independent Earth rotation measurements utilizing the techniques of optical astrometry, very long baseline interferometry (VLBI) and lunar laser ranging (LLR). For the atmospheric angular momentum, National Center for Environmental Prediction (NCEP) Reanalyses for the period 1958 - 1998 [*Kalnay et al.*, 1997] are investigated with 5-day averages being considered. Zonal wind contributions up to the 10 hPa level are included in the global analysis; for the latitudinally belted analysis, zonal winds up to 100 hPa are considered in order to make the distinction between tropospheric and stratospheric quasi-biennial oscillations (the former being linked to the ENSO phenomenon).

For the SOI, we use here a modified version of the Southern Oscillation Index based on monthly Tahiti and Darwin sea level pressure (SLP) data, provided by the National Center

for Environmental Prediction. The time series is obtained here by first removing the composite annual cycle (this is done by subtracting from both time series the mean SLP value at that location for the corresponding month), dividing the monthly anomalies so obtained by the corresponding standard derivation, and then taking the Darwin-minus-Tahiti differences. Note that the series used here, the "Modified Southern Oscillation Index" (MSOI), differs from the SOI by the fact that it is opposite in sign to the usually defined SOI (e.g. *Trenberth and Shea*, 1987), so as to be positively correlated with the LOD (see Fig. 2).

Analyses utilize both a recursive filter [*Murakami*, 1979] and singular spectrum analysis (SSA) in both its single channel and multi-channel modes. SSA is algorithmically equivalent to the application of extended empirical orthogonal functions (EEOFs) [e.g. *Weare and Nasstrom*, 1982] to a univariate time series but has special features and greater flexibility when applied to the analysis of phenomena with longer time scales and higher sampling rates. The purpose of using the Multi-channel Singular Spectral Analysis (MSSA) is to clarify further the spatial patterns associated with the regular, nearly periodic components of the El Nino Southern Oscillation. The built-in advantage of MSSA as defined by *Plaut and Vautard* [1994] is to account for both space and time correlations, and to characterize traveling and/or standing oscillations. The main interest here of using MSSA is to determine the global/planetary characteristics of the low-frequency zonal flow patterns associated with ENSO; MSSA is directly applied on the latitudinally-banded AAM and the results plotted in a Hovmoeller diagram.

Analysis and Discussion

Since the focus of the current paper is the most recent ENSO event, it is imperative to extract the longer term decadal signal present in the LOD series (Fig. 1a), which is believed to result mostly from slow variations in the angular momentum of the Earth's liquid outer core (e.g. *Hide and Dickey*, 1991). First, we account for the strong seasonal terms in LOD and AAM by removing the composite annual cycle (which is computed as a multiyear average at each pentad of the year). The remaining LOD and AAM signals are shown in Fig. 1a and 1b respectively. By taking the difference between the LOD and AAM (Fig. 1c, dotted line) we obtain the LOD variations unexplained by angular momentum exchange with the atmosphere, i.e. rotational variations excited by other sources such as changes in core angular momentum (CAM) and oceanic angular momentum (OAM). We assume that the long term trend of LOD-AAM is dominated by angular momentum exchange between the Earth's mantle and the core; however, it may also contain small contributions from

other angular momentum reservoirs. The variability due to core angular momentum (Fig. 1c, solid line), i.e. the longer term behavior of LOD-AAM, was determined by SSA using an embedding dimension taken near to its recommended maximum (9 years, i.e. one third of the dataspan [*Vautard et al.,* 1992]); the first five eigenvalues contribute significantly to the long term variation. Subtracting this SSA-determined CAM from LOD leads to a residual LOD series (Fig. 1d), with its composite annual cycle and decadal signal removed, which displays both strong interannual as well as intraseasonal variabilities.

A comparison among AAM, LOD and MSOI (Fig. 2) indicates remarkable agreement, with the dashed lines representing the analyzed data and the full lines the leading modes from a joint M-SSA analysis. Note the strong peaks evident in 1982-83 and in 1997-98. The most intense part of the 1982-83 event has large positive amplitude (0.9 for LOD and AAM, and 0.8 for MSOI), rather short duration (approximately 4 months) and is centered around a robust peak in January 1983. In contrast, the most recent event is quite broad, beginning in early 1997 and abruptly changing into a La Nina event in Spring 1998. The maximum amplitude of the unfiltered series is 15-20% lower than is the case for the 1982-83 event. While the recent LOD/AAM maximum have a long duration (~1 yr) they are punctuated by higher-frequency bursts, possibly associated with enhanced activity of the Madden-Julian oscillation [*Yu and Rienecker*, 1998]. The 1988-89 La Nina event is clearly evident in the all three data types as a pronounced minimum; the anomalous prolonged El Nino activity in the early to mid-1990's appears as a broad maxima in all three series, modulated by ripples on a QB time scale.

Additional insight into the origin of interannual rotational fluctuations can be gained through the examination of the latitudinal structure of the associated atmospheric variation [*Dickey et al.*, 1992; *Black et al.*, 1996]. The AAM obtained by integrating atmospheric wind data up to 100 hPa over 46 equal-area belts is considered, with interannual variations obtained using a recursive filter [*Murakami*, 1979] with three different ranges: ENSO band (20-70 months; see Fig. 3a), low frequency band (LF-37-70 months; see Fig. 3b), and the quasi-biennial band (QB-20-38 months; see Fig. 3c).

The M-SSA technique is also applied; here the latitudinally belted data are combined into 23 equal areas for computational efficiency, with each of the belts considered as a separate channel in the joint analysis. An embedding dimension (window length) of 5 years was chosen in order to include oscillations which have roughly apparent periods between 1 window length and 1/5 of the window length [*Vautard et al.*, 1992], that is to obtain

optimal representation of both the quasi-biennial and low-frequency bands. The twenty-three channels were each decimated by a factor 4 (one sample every 20 days). The LF and QB components (with the LF being the larger of two) are each represented by one pair of eigenvalues in the MSSA results, indicating the oscillatory nature of these phenomena. This is analogous to the Fourier transform, for which two eigenfunctions (sine and cosine) in quadrature are needed to represent a purely periodic signal. In the case of MSSA, the two eigenfunctions are orthogonal, in quadrature, and paired but are not restricted to a uniform frequency or amplitude. We define the quasi-biennial oscillation and the low-frequency oscillation to be the reconstructed components [cf. *Vautard et al.,* 1992] from their respective QB and LF pairs of eigenfunctions and principal components [see Fig. 3d-f, where 3f (the ENSO band) is their sum].

The resulting pattern of interannual variability is manifest in both analyses, with V-like structures emerging from the tropics and propagating poleward. The recursive filtering is applied independently on each equal-area belt (Fig. 3a-c). Although correlations between belts are not taken into account within this approach, coherent poleward propagation patterns are obvious. Low-frequency variability associated with latitude-specific events is still visible, however, and tends to obscure the underlying pattern during periods when ENSO is less active. By contrast, MSSA is designed to isolate patterns of variability which are coherent between the different channels (i.e. latitude belts), making this technique especially well suited to detect global-scale oscillations linked to the ENSO cycle. Note the decadal modulation of the signal evident in both analyses. Enhanced activity is observed in the ENSO band between ~1967-1976 and again from ~1981-1990, as well as the present epoch (since 1997); in the intervening epochs the propagation pattern is less visible in the recursively-filtered results, where each belt is analyzed separately. There is a rather abrupt change in the propagation pattern at ~ 45^0 North in all three bands, which is especially evident in the MSSA analysis.

Focusing in on particular events, the 1982-1983 event is associated with positive AAM (that is anomalous eastward winds) beginning at the equator in late 1981/early 1982 and propagating to high latitudes in both hemispheres over the course of several years. During the mature phase of the ENSO event (late 1982 to early 1983), strong positive anomalies are located in the northern subtropics with moderate anomalies in the southern subtropics. These anomalies diminish in strength and propagate poleward as the ENSO events decays. A similar scenario can be seen for the 1972-73 event, which also shows a strong signal of poleward propagation. The strong ENSO events in 1972-73, 1982-83 and 1997-98 are

especially robust with additional less pronounced episodes in 1977 and 1987. Not all of the propagating structures are associated with ENSO events, however. Due to the V-like signature of poleward propagation evident in the Hovmoller diagrams, in particular, interannual variations in the total AAM (which is strongly correlated with the SOI, cf. Fig. 1) may be reduced as the result of cancellations between zonal flows in the tropics, mid-latitudes and polar regions. For example, westerly anomalies during 1979-80 are quite strong in the tropics and in the northern hemisphere extratropics, but concomitant strong easterly anomalies in the southern hemisphere extratropics have an offsetting effect, with the resultant AAM sum not being of sufficient magnitude to be classified an ENSO event.

Turning to the recent (1997-1998) event, a V-like structure is visible in both analyses; while the M-SSA results largely depict the time-variance of the dominant propagation pattern, the recursive results show that coherent westerly anomalies actually began in the summer of 1996 in the LF band and in late 1996 in the QB band. Constructive interference is evident in the ENSO band (Fig. 3a), with strong tropical activity in early 1997 propagating poleward to produce enhanced activity in the mid-latitudes in late 1997/early 1998. By the beginning of 1998, signs of the coming La Niña event were already evident, with easterly anomalies developing in the tropics. Unlike the 1982-83 event [*Rosen et al.*, 1984], which had dominant AAM maxima in the mid-latitudes, the current event has more activity in the tropics; in this regard, the current event is more comparable to the 1972-73 event.

Concluding Remarks

The effect of the most recent 1997-98 ENSO event is clearly evident in the length of day, and is highly correlated with strong signatures in the Southern Oscillation Index and in the atmospheric angular momentum. Examining AAM anomalies in equal area latitudinal belts, a coherent poleward propagating signature originating in the tropics is observed, consistent with V-like patterns found during earlier El Ninos; indications of the subsequent La Niña event are apparent in the emergence of easterly anomalies in the tropics in early 1998.

Acknowledgments

The authors gratefully acknowledge Prof. M. Ghil for many beneficial discussions, Prof. R. Vautard for the supplying the M-SSA software used in this analysis, and Drs. R.S. Gross and J.T. Ratcliff making available the 1998 operational LOD series. This paper presents the results of one phase of research carried out at the Jet Propulsion Laboratory,

California Institute of Technology, sponsored by the National Aeronautics and Space Administration (NASA) and National Oceanic and Atmospheric Administration (NOAA).

Figure Captions

Fig. 1 (a) The Kalman-filtered length-of-day (LOD) data (COMB97 - *Gross*, 1998) with composite annual cycle removed, (b) NCEP reanalysis atmospheric angular momentum (AAM) with composite annual cycle removed, (c) the difference between LOD and AAM (both with composite annual cycle removed) shown with curve representing decadal core effects obtained using Singular Spectrum Analysis (SSA), and (d) LOD with composite annual cycle and decadal signal removed.

Fig. 2 A comparison among LOD, AAM, and MSOI (a, b, and c, respectively). The AAM series is expressed in equivalent LOD units (i.e. milliseconds), and the MSOI series has been scaled to have the same standard deviation as the LOD. The strong 1982-83 and 1997-87 El Nino as well as the current La Nina are clearly evident. The dashed lines represent the processed data, whereas the full lines are the results of the leading modes of multi-channel singular spectrum analysis.

Fig. 3 Latitude-time (Hovmöller) plot of interannual atmospheric angular-momentum variations. We use the series of the NCEP reanalysis series integrated over 46 separate equal-area latitude bands based on atmospheric wind data up to 100 mbar. Interannual variation obtained by recursive-filtering in the three interannual bands: ENSO band (20-70 months (a)); the low-frequency (LF) band (37-70 months (b)); and the quasibiennial (QB) band (20-38 months (c)). In addition, the corresponding results [(d) - (f)] are shown from the multi-channel singular spectrum analyses. The numerical scale represents the LOD anomaly (in microseconds) which would result if the global atmosphere (i.e. sum at all the belts) had the same anomalous AAM as the individual belt at which the anomaly is plotted.

References:

Black, R. X., D. A. Salstein, R. D. Rosen, Interannual Modes of Variability in Atmospheric Angular-Momentum, *Journal of Climate* , **9** (11): pp. 2834-2849, 1996.

Chao, B. F., Interannual length-of-day variation with El Nino/Southern Oscillation/El Nino, *Geophys. Res. Lett.*, **11**, 541-544, 1984.

Chao, B. F., Correlation of interannual length-of-day variations with El Nino/Southern Oscillation, 1972-1986, *J. Geophys. Res.*, **93,** 7709-7715, 1988.

Chao, B. F., Length-of-day variations caused by El Nino/Southern Oscillation and the quasi-biennial oscillation, *Science,* **243,** 923-925, 1989.

Dickey, J. O., S. L. Marcus, and R. Hide, Global Propagation of Interannual Fluctuations in Atmospheric Angular Momentum, *Nature*, **357**, 484-488, 1992.

Dickey, J. O., S. L. Marcus, T. M. Embanks, and R. Hide, Climate studies via space geodesy: Relationships between ENSO and interannual length-of-day variations, in *Interactions Between Global Climate Subsystems: The Legacy of Hann, Geophys. Monogr. Ser.,* vol. 75, edited by G. A. McBean and M. Hantel, pp. 141-155, AGU, Washington, D. C., 1993.

Dickey, J. O., S. L. Marcus, R. Hide, T. M. Eubanks, and D. H. Boggs, Angular Momentum Exchange Among the Solid Earth, Atmosphere, and Oceans--A Case Study of the 1925-86, *J. Geophys. Res.*, **99**, 23,921-23937, 1994.

Eubanks, T. M., J. A. Steppe, and J. O. Dickey, The El Nino, the Southern Oscillation and the Earth's Rotation, in *Earth Rotation: Solved and Unsolved Problems, NATO Advanced Institute Series C: Mathematical and Physical Sciences,* **187**, ed. A. Cazenave, 163-186, D. Reidel, Hingham, Mass., 1986.

Hide, R. and J.O. Dickey, The Earth's variable rotation, *Science*, **253**, 629-637, 1991.

Gambis, D., Wavelet Transform Analysis of the Length of the Day and the El Nino/Southern Oscillation Variations at Intraseasonal and Interannual Time Scales, *Ann. Geophys,* **10**, 429-437,1992.

Gross, R. S., T. M. Eubanks, J. A. Steppe, A. P. Freedman, J. O. Dickey, and T. F. Runge, A Kalman filter-based approach to combining independent Earth orientation series, *J. Geodesy*, 72, 215-235, 1998.

Kalnay, E., M. Kanamitsu, R. Kistler, W. Collins, D. Deaven, L. Gandin, M. Iredell, S. Saha, G. White, *et al.*, The NCEP/NCAR 40-year reanalysis project, *Bull. Amer. Met. Soc.*, **77** (3), pp. 437-471, 1996.

McPhaden, M.J., The 1997 - 1998 El Nino in Review: Lessons and Challenges for Climate Research, *Eos, Trans. AGU 49(45),* Fall Meet. Suppl., 493, 1998

Murakami, M., Large-scale aspects of deep convective activity over the GATE area, *Mon. Weather Rev.*, **107**, 994-1013, 1979.

Rosen, R. D., D. A. Salstein, T. M. Eubanks, J. O. Dickey, and J. A. Steppe, An El Nino signal in atmospheric angular momentum and Earth rotation, *Science*, **225**, 411-414, 1984.

Salstein, D. A., and R. D. Rosen, Earth rotation as a proxy for interannual variability in atmospheric circulation, 1860-present, *J. Clim. Appl. Meteorol.*, **25**, 1870-1877, 1986.

Trenberth, K. E., and D. J. Shea, On the Evolution of the Southern Oscillation, *Mon. Weather. Rev.*, **115**, 3078-3096, 1987.

Vautard, R., P.Yiou, and M. Ghil, Singular spectrum analysis: A toolkit for short noisy chaotic signals, *Phys. D Amsterdam*, **58**, 95-126, 1992.

Weare, B.C. and J.S. Nasstrom, Examples of extended empirical orthogonal function analyses, *Mon.Weath. Rev.*, **110**, 481 - 485, 1982.

Yu, L., and M. M. Rienecker, Evidence of an extratropical influence during the onset of the 1997-98 El Niño, **25**, 3537-3540, 1998.

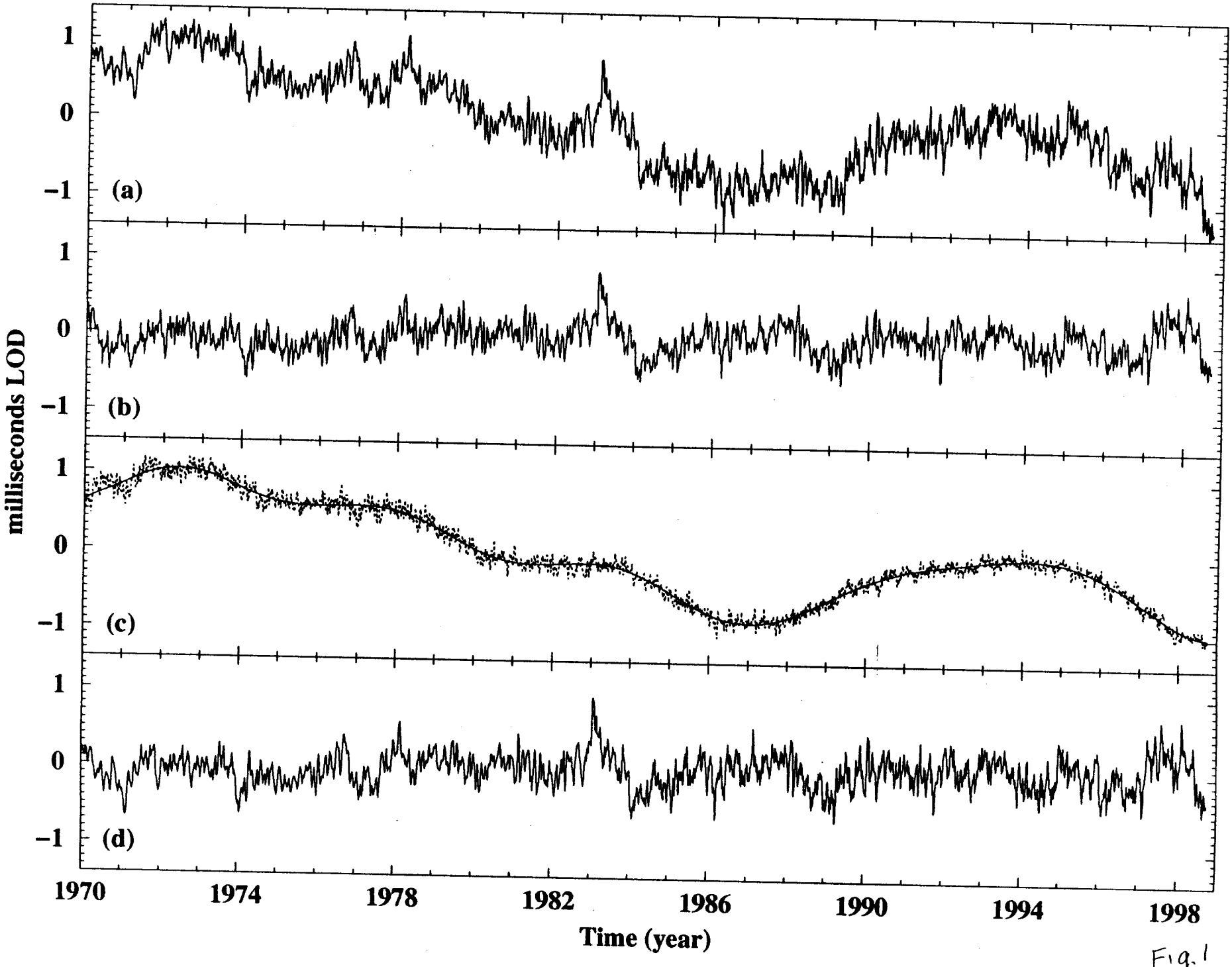
1
0
−1
(a)
(b)
(c)
(d)
milliseconds LOD
1970
1974
1978
1982
1986
1990
1994
1998
Time (year)

Fig. 1

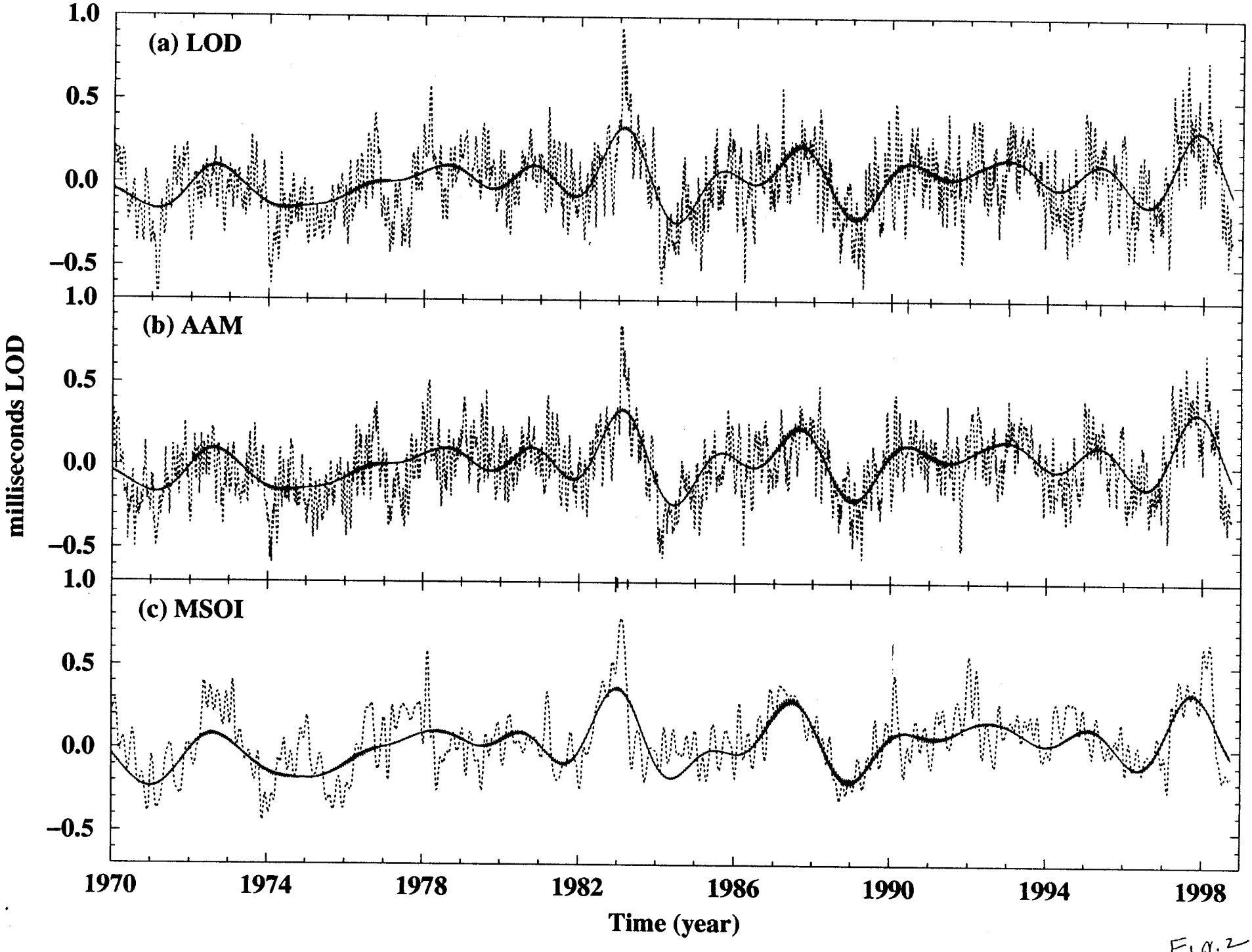
(a) LOD
(b) AAM
(c) MSOI
1.0
0.5
0.0
−0.5
milliseconds LOD
1970
1974
1978
1982
1986
1990
1994
1998
Time (year)

Fig. 2

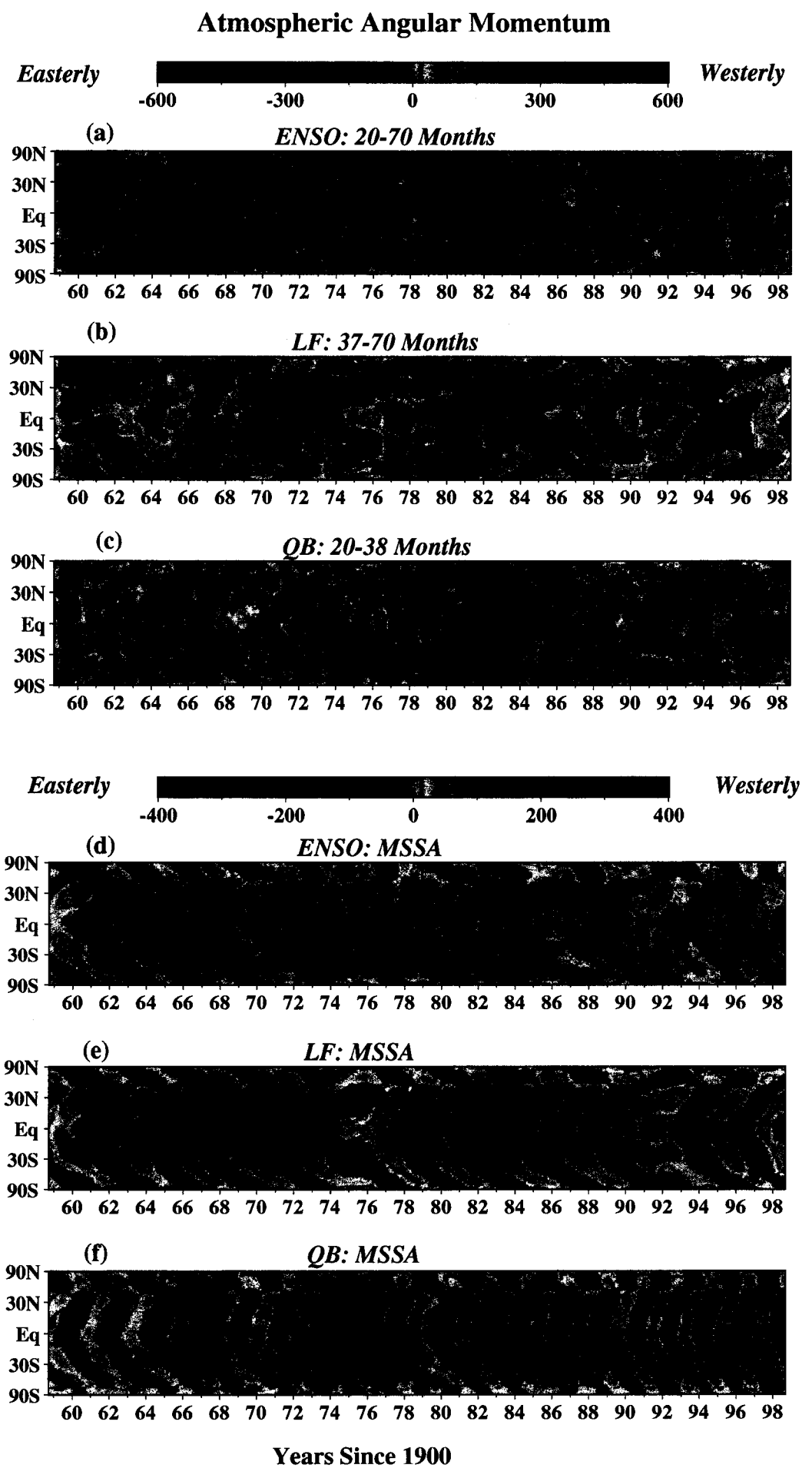
Atmospheric Angular Momentum
Easterly
Westerly
-600
-300
0
300
600
(a)
ENSO: 20-70 Months
(b)
LF: 37-70 Months
(c)
QB: 20-38 Months
-400
-200
0
200
400
(d)
ENSO: MSSA
(e)
LF: MSSA
(f)
QB: MSSA
90N
30N
Eq
30S
90S
60 62 64 66 68 70 72 74 76 78 80 82 84 86 88 90 92 94 96 98
Years Since 1900